CHAPTER V

IDENTIFICATION OF ELLAGIC ACID ANALOGUES AS POTENT INHIBITOR OF PROTEIN KINASE CK2: A CHEMOPREVENTIVE ROLE IN ORAL CANCER

5. INTRODUCTION

Protein kinase CK2 is a highly ubiquitous and conserved protein serine/threonine kinase that has been found to be involved not only in cell growth and proliferation, but also in suppression of apoptosis in cells. CK2 is capable of dynamic intracellular shuttling in response to a variety of signals. It is localized in both the nucleus and cytoplasm in normal cells, but is particularly predominant in the nuclear compartment in cancer cells. CK2 has been found to be uniformly deregulated in all the cancers that have been examined. Down regulation of CK2 by chemical or molecular methods promotes apoptosis in cells (Ahmad *et al*., 2005). It has been reported that antisense CK2 alpha is particularly potent in inducing apoptosis in cancer cells in culture as well as in xenograft models of cancer such as oral cancer and squamous cell carcinoma of head and neck (Ahmad *et al*., 2005).

Ellagic acid is a naturally occurring phenolic constituent present in fruits and nuts. Whether the various pharmacological properties attributed to ellagic acid are due to ellagic acid alone or its metabolites, or the combination of both, are still not precisely known. The anti-proliferative properties of ellagic acid are due to its ability to directly inhibit the DNA binding of certain carcinogens, including polycyclic aromatic hydrocarbons (Teel *et al.*, 1986)

and nitrosamines (Mandal *et al.*, 1988; Mandal and Stoner, 1990; Siglin *et al.*, 1995). Ellagic acid down-regulates insulin-like growth factor (IGF-II) (Narayanan and Re, 2001) and activates expression of tumor suppressor genes p53/p21, leading to cell cycle arrest at the G1/S phase and apoptosis (Narayanan *et al.*, 1999). Ellagic acid prevents carcinogen induced tumorigenesis by activating detoxifying enzymes (Barch and Rundhaugen, 1994) and inhibiting certain cytochrome P450 enzymes involved in the generation of mutagens (Zhang *et al.*, 1993, Barch *et al.*, 1994). Anticarcinogenic effect of ellagic acid has been reported in prostate (Narayanan *et al.*, 2002), liver (Tanaka *et al.*, 1988), colorectal (Narayanan and Re, 2001), esophageal (Stoner *et al.*, 1999), bladder (Li *et al.*, 2005) and leukemia (Mertens-Talcott and Percival 2005, Hagiwara *et al.*, 2010) cancer cell lines. Ellagic acid was reported to reduce chemotherapy induced toxicity in hormone refractory prostate cancer (HRPC) (Falsaperla *et al.*, 2005). Ellagic acid was reported to inhibit 4-nitroquinoline-1-oxide (4-NQO)-induced tongue carcinogenesis in rat (Tanaka *et al.*, 1993) and inhibit the growth of premalignant and malignant oral human cell-line (Han *et al.*, 2005).

Several research studies have identified Ellagic acid as a potent anticarcinogenic and antimutagenic compound (Narayanan and Re, 2001). At present, ellagic acid represents the most potent known CK2 inhibitor (Ki = 20 nM). Using a virtual screening approach, I have screened several ellagic acid analogues with high chemical diversity and molecular specificity, as these novel potent CK2 inhibitors.

5.1 MATERIALS AND METHODS

5.1.1 Receptor X-ray structure

The Protein Data Bank (PDB) is a repository for the 3D structural data of large biological molecules, such as proteins and nucleic acids. The data typically obtained by X-ray crystallography or NMR spectroscopy can be accessed at http://www.rcsb.org. The 3D coordinates of the crystal structure of human CK2 alpha complex with ellagic acid (PDB id: 2ZJW) was retrieved from PDB and taken as the receptor model in flexible docking program. Chimera is a highly extensible program for interactive visualization, analysis of molecular structures and related data, including density maps, super-molecular assemblies, sequence alignments, docking results, trajectories and conformational ensembles. Human casein kinase II (CK2) was optimized by chimera tool (Falsaperla, *et al.,* 2005). Before docking heteroatom Ellagic acid (REF) was removed from .PDB file of CK2 (PDB id: 2ZJW) by charge method AMI-BCC using chimera. After removing the water molecule, hydrogen atom were added to protein for correct ionization and tautomeric states of amino acid residues such as Asp, Ser, Glu, Arg and His.

5.1.2 Active site analysis

The active site residues of human casein kinase II (CK2) was taken from the PDBSUM entry of 2ZJW having binding site residues ASP175, PHE113, LYS68, ILE174, ILE95, VAL66, VAL53 and LEU45 for inhibitor Ellagic acid (2,3,7,8-tetrahydroxychromeno[5,4,3-cde]chromene-5,10-dione).

5.1.3 Inhibitors Dataset

The data regarding the experimentally known 38 coumarin and alike inhibitors of CK2, classified as potent, moderate and slightly weak, was obtained from the literature (Chilin *et al.*, 2008). The 3D structures of known 38 inhibitors were downloaded in .sdf format from pubchem compound database. They were later converted in .pdb format by the help of open babel (Riggs *et al.,* 2006) software. Babel is a cross-platform program designed to converts chemical objects (currently molecules) from one file format to another. This chemical toolbox is used in molecular modeling, computational chemistry and related areas to convert, analyze, or store data. Figure 5.1 shows the Interface of Babel Molecular format converter for converting .sdf format to .pdb format is shown below:

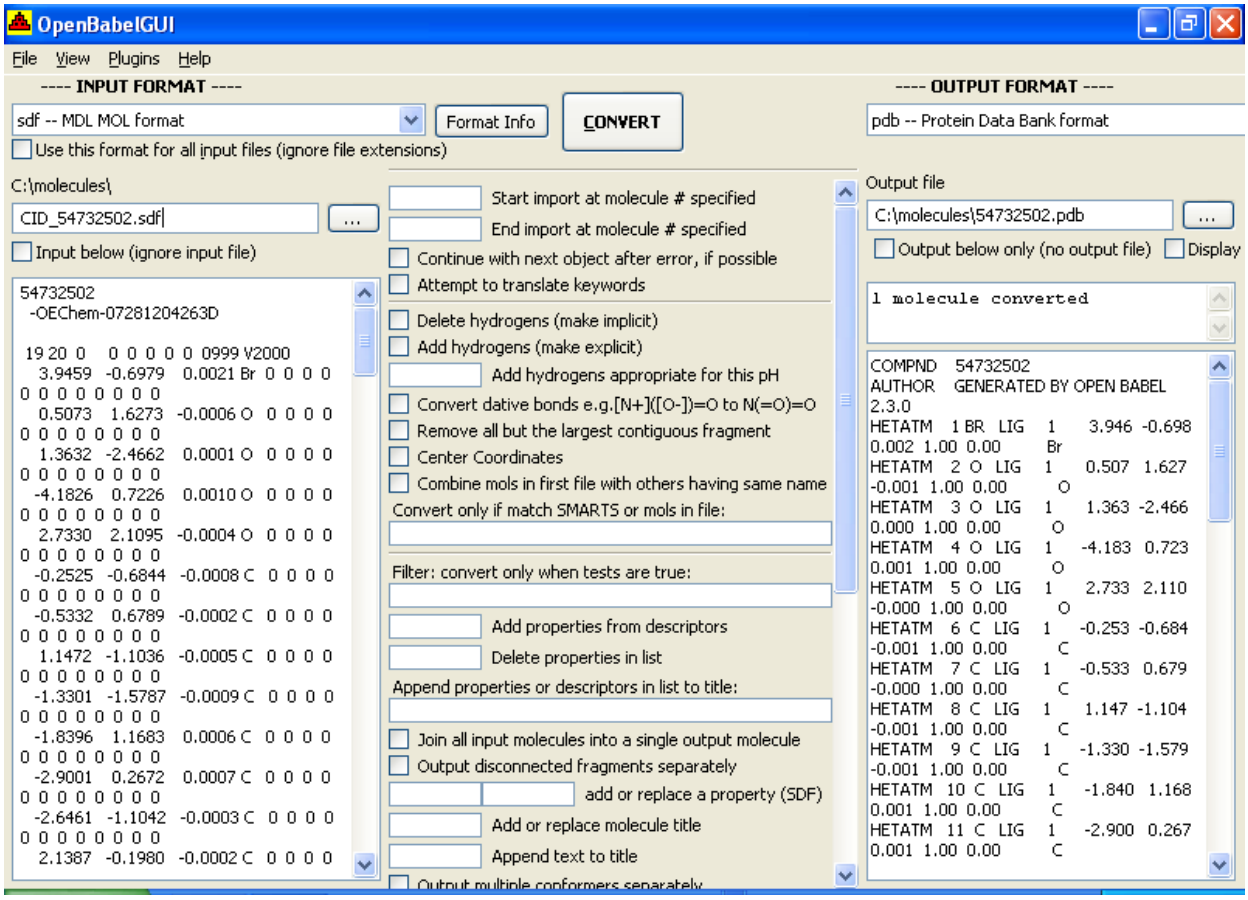

Figure 5.1: Input format of Babel Molecule Format Converter.

The 2D structure and IC50 (50% inhibitory concentration) value of coumarin inhibitors are shown in Table 5.1.

Table 5.1: List of inhibitors known to be active against CK2.

Sl. N0.	CID No.	Structure	IUPAC Name	Exp. IC_{50} (µM)	MWT (g/mol)	Molecular formula	X Log P	HBD	HBA
1.	54732502	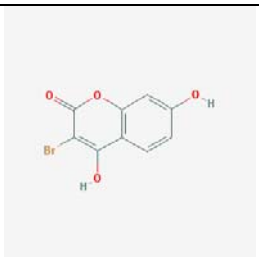	3-bromo-4,7-dihydroxychromen-2-one	39	257.0376	$C_9H_5BrO_4$	1.8	2	4
2	54682226	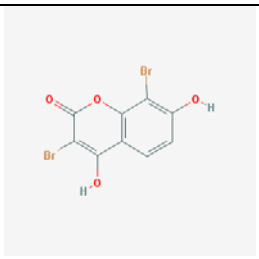	3,8-dibromo-4,7-dihydroxychromen-2-one	28	335.93366	$C_9H_4Br_2O_4$	2.5	2	4
3	44456889	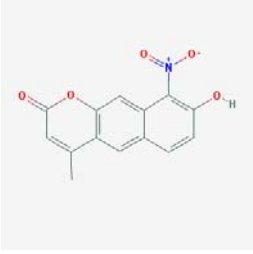	8-hydroxy-4-methyl-9-nitrobenzo[g]chromen-2-one	0.3	271.22496	$C_{14}H_9NO_5$	3.1	1	5
4	44456746	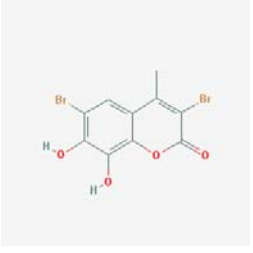	3,6-dibromo-7,8-dihydroxy-4-methylchromen-2-one	3.6	349.96024	$C_{10}H_6Br_2O_4$	2.7	2	4

5	44456745		3-bromo-7-hydroxy-4-methyl-6-nitrochromen-2-one	3.3	300.06234	$C_{10}H_6BrNO_5$	2.8	1	5
6	44456744	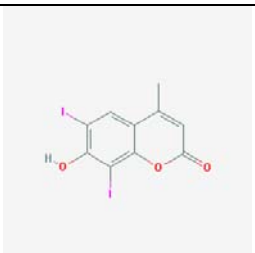	7-hydroxy-6,8-diiodo-4-methylchromen-2-one	2.66	427.96178	$C_{10}H_6I_2O_3$	2.8	1	3
7	44456718	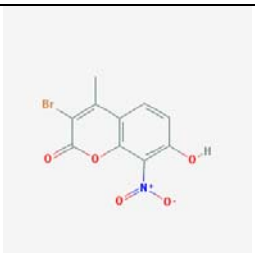	3-bromo-7-hydroxy-4-methyl-8-nitrochromen-2-one	4	300.06234	$C_{10}H_6BrNO_5$	2.8	1	5
8	44456717	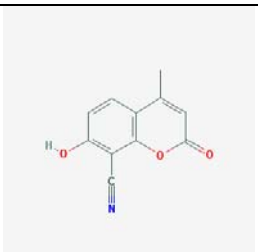	7-hydroxy-4-methyl-2-oxochromene-8-carbonitrile	4.2	201.17818	$C_{11}H_7NO_3$	1.7	1	4
9	44456698	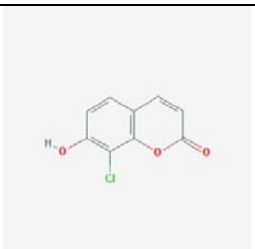	8-chloro-7-hydroxychromen-2-one	10.7	196.5872	$C_9H_5ClO_3$	2.2	1	3
10	44456697	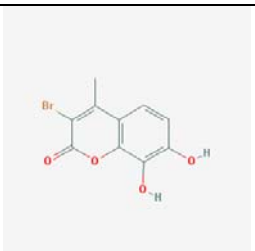	3-bromo-7,8-dihydroxy-4-methylchromen-2-one	10.5	271.06418	$C_{10}H_7BrO_4$	2	2	4

11	44456695	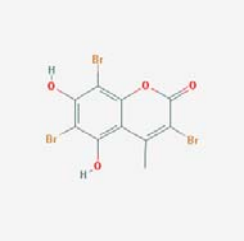	3,6,8-tribromo-5,7-dihydroxy-4-methylchromen-2-one	21.5	428.8563	$C_{10}H_5Br_3O_4$	3.4	2	4
12	44456694	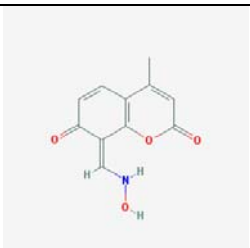	(8E)-8-[(hydroxyamino)methylidene]-4-methylchromene-2,7-dione	20	219.19346	$C_{11}H_9NO_4$	0.5	2	5
13	44456692	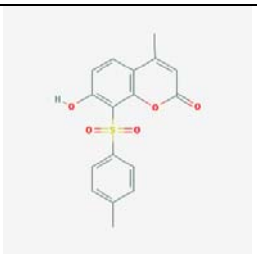	7-hydroxy-4-methyl-8-(4-methylphenyl)sulfonylchromen-2-one	22.7	330.35506	$C_{17}H_{14}O_5S$	3.2	1	5
14	44456668	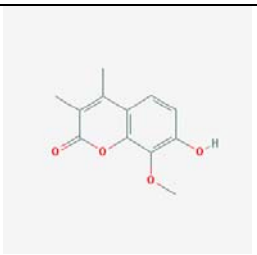	7-hydroxy-8-methoxy-3,4-dimethylchromen-2-one	27	220.22128	$C_{12}H_{12}O_4$	1.8	1	4
15	44456667	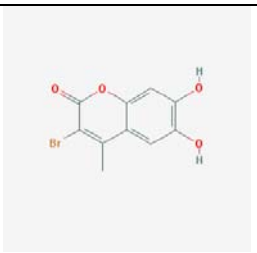	3-bromo-6,7-dihydroxy-4-methylchromen-2-one	31	271.06418	$C_{10}H_7BrO_4$	2	2	4
16	24799273	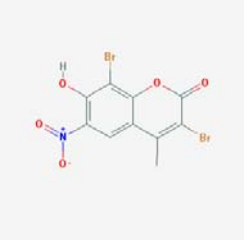	3,8-dibromo-7-hydroxy-4-methyl-6-nitrochromen-2-one	4	378.9584	$C_{10}H_5Br_2NO_5$	3.4	1	5

17	24799272	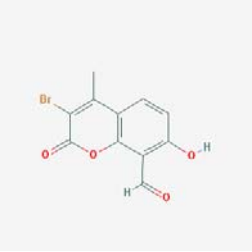	3-bromo-7-hydroxy-4-methyl-2-oxochromene-8-carbaldehyde	3.3	283.07488	$C_{11}H_7BrO_4$	2.4	1	4
18	24799271	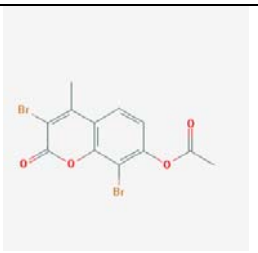	(3,8-dibromo-4-methyl-2-oxochromen-7-yl) acetate	2.5	375.99752	$C_{12}H_8Br_2O_4$	3.2	0	4
19	24799269	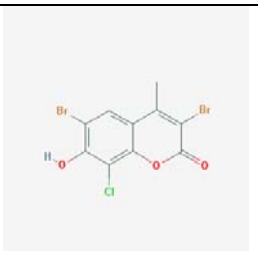	3,6-dibromo-8-chloro-7-hydroxy-4-methylchromen-2-one	4.03	368.4059	$C_{10}H_5Br_2ClO_3$	3.7	1	3
20	24799087	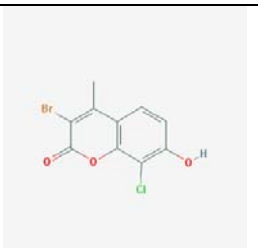	3-bromo-8-chloro-7-hydroxy-4-methylchromen-2-one	.32	289.50984	$C_{10}H_6BrClO_3$	3	1	3
21	24799086	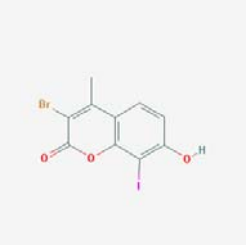	3-bromo-7-hydroxy-8-iodo-4-methylchromen-2-one	0.28	380.96131	$C_{10}H_6BrIO_3$	3	1	3
22	24799081	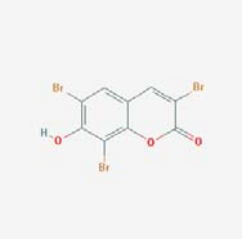	3,6,8-tribromo-7-hydroxychromen-2-one	15.21	398.83032	$C_9H_3Br_3O_3$	3.8	1	3

23	24799080	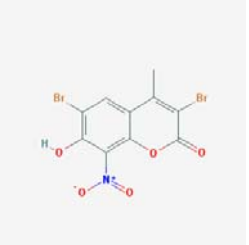	3,6-dibromo-7-hydroxy-4-methyl-8-nitrochromen-2-one	4	378.9584	$C_{10}H_5Br_2NO_5$	3.4	1	5
24	24799079	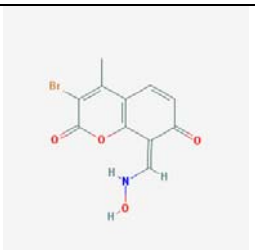	(8E)-3-bromo-8-[(hydroxyamino)methylidene]-4-methylchromene-2,7-dione	2.5	298.08952	$C_{11}H_8BrNO_4$	1.4	2	5
25	20144512	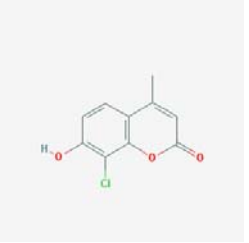	8-chloro-7-hydroxy-4-methylchromen-2-one	2.2	210.61378	$C_{10}H_7ClO_3$	2.1	1	3
26	15686455	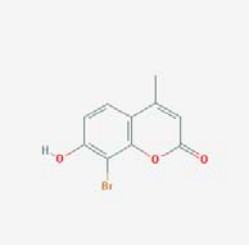	8-bromo-7-hydroxy-4-methylchromen-2-one	0.74	255.06478	$C_{10}H_7BrO_3$	2.2	1	3
27	15445625	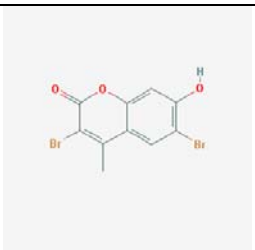	3,6-dibromo-7-hydroxy-4-methylchromen-2-one	.66	333.96084	$C_{10}H_6Br_2O_3$	3.1	1	3
28	13881279	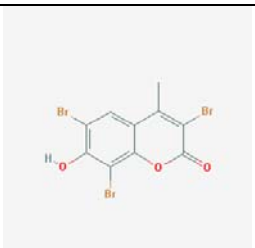	3,6,8-tribromo-7-hydroxy-4-methylchromen-2-one	1.9	412.8569	$C_{10}H_5Br_3O_3$	3.8	1	3

29	11087876		3-bromo-7-hydroxy-8-methyl-6-nitrochromen-2-one	35	300.06234	$C_{10}H_6BrNO_5$	3.2	1	5
30	5795340	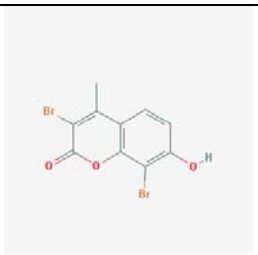	3,8-dibromo-7-hydroxy-4-methylchromen-2-one	.1	333.96084	$C_{10}H_6Br_2O_3$	3.1	1	3
31	5417177	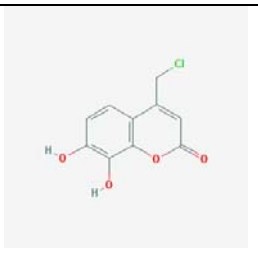	4-(chloromethyl)-7,8-dihydroxychromen-2-one	4	226.61318	$C_{10}H_7ClO_4$	1.1	2	4
32	5415301	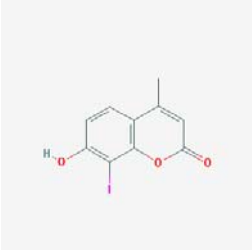	7-hydroxy-8-iodo-4-methylchromen-2-one	.8	302.06525	$C_{10}H_7IO_3$	2.1	1	3
33	5385113		7-hydroxy-4-methyl-6-nitrochromen-2-one	30	221.16628	$C_{10}H_7NO_5$	2.3	1	5
34	5376327	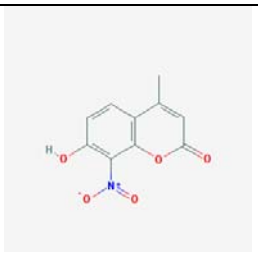	7-hydroxy-4-methyl-8-nitrochromen-2-one	4	221.16628	$C_{10}H_7NO_5$	1.8	1	5

35	5354284	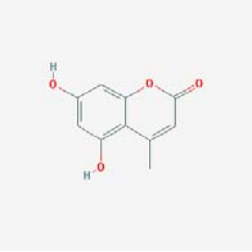	5,7-dihydroxy-4-methylchromen-2-one	34.96	192.16812	$C_{10}H_8O_4$	1.1	2	4
36	5324654	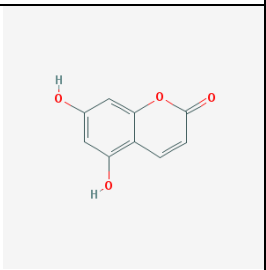	5,7-dihydroxychromen-2-one	34.96	178.14154	$C_9H_6O_4$	1.2	2	4
37	5291935	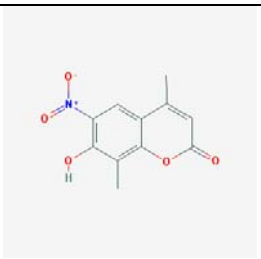	7-hydroxy-4,8-dimethyl-6-nitrochromen-2-one	30	235.19286	$C_{11}H_9NO_5$	2.2	1	5
38	5281855	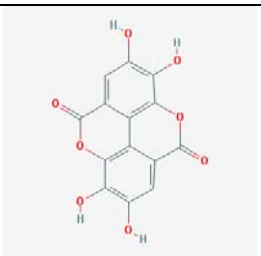	2,3,7,8-tetrahydroxychromeno[5,4,3-cde]chromene-5,10-dione	0.04	302.19264	$C_{14}H_6O_8$	1.1	4	8

MWT: Molecular weight; HBD: Hydrogen bond donor; HBA: Hydrogen bond acceptor

5.1.4 Molecular Docking

AutoDock 3.0.5 is a suite of automated docking tools used to predict how small molecules such as substrate, ligand or drug candidates, bind to a receptor of known 3D structure. This enables us significant insights into molecular recognition and network interactions such as signal transduction pathways in cells. To assist in studying protein interactions, autodock 3.0.5 programs were considered for protein-ligand docking which is shown below in the

figure 5.2. AutoDock actually consists of two main programs: autodock and autogrid. AutoDock performs the docking of the ligand to a set of grids describing the target protein; AutoGrid pre-calculates these grids (http://autodock.scripps.edu).

AutoDock 3.0.5 is parameterized to use a model of the protein and the ligand that includes polar hydrogen atoms, but not the hydrogen atoms which are bonded to carbon atoms. An extended format of the .PDB, known as PDBQS, is used for coordinate files, which includes atomic partial charges and atom types. The current AutoDock force field uses several atom types for the most common atoms, including separate types for aliphatic and aromatic carbon atoms, and separate types for polar atoms that form hydrogen bonds and those that do not form hydrogen bonds.

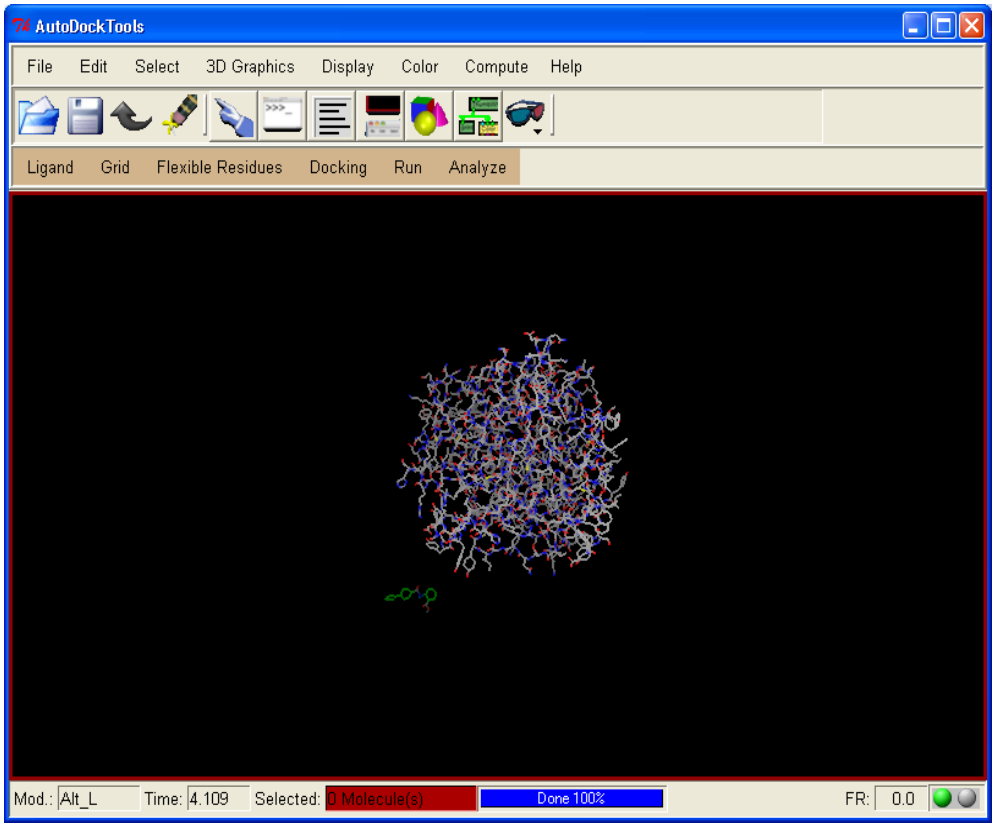

Figure 5.2: Interaction of ligand with protein by the help of Autodock tools.

AutoDock tools detect whether the ligand already has charges or not. If not, AutoDock tools determine whether the ligand is a peptide, by checking all of its residues names appear in the standard set of the 20 commonly occurring amino acids. If all the residues are amino acids, AutoDock tool adds Kollman charges to the ligand. If not, then it computes Gasteiger charges; it is essential that for the Gasteiger calculation to work correctly, the ligand must have all the hydrogen atoms added, including both the polar and non-polar ones. If the charges are all zero, then AutoDock tools try to add charges. It checks whether the total charge per residue is an integer. Kollman charges are added up using a look-up dictionary based on the names of the atoms in the ligand. If the name is not found, a charge of 0.0 is assigned (Castrignano *et al*., 2006).

Docking of 38 inhibitors screened from literature against CK2 structure was done using molecular docking program AutoDock 3.0.5 (Goodsell *et al*., 1996). Gasteiger charges were added to the ligand and maximum 6 numbers of active torsions were given to the lead compounds using AutoDock tool (Morris *et al.,* 1998). Kollman charges and the solvation term were then added to the protein structure using the same. I have made the grid and adjusted the number of points in X, Y, Z-axis so that the entire active site residues (ASP175, PHE113, LYS68, ILE174, ILE95, VAL66, VAL53 and LEU45) of the human casein kinase II (CK2) were covered. The default value was 0.375 Å between grid points, which was about a quarter of the length of a carbon-carbon single bond. The spacing between grid points could be adjusted with another thumbwheel. Grid spacing values of up to 1.0 Å could be used when a large volume is to be investigated. The Lamarckian genetic algorithm implemented in Autodock was used. Docking parameters were as follows: 30 docking trials, population size

of 150, maximum number of energy evaluation ranges of 25,0000, maximum number of generations is 27,000, mutation rate of 0.02, cross-over rate of 0.8, Other docking parameters were set to the software's default values. After docking, the ligands were ranked according to their docked energy as implemented in the AutoDock 3.0.5 program.

5.1.5 Cygwin

Cygwin (http://www.cygwin.com/) is a collection of free software tools originally developed by Cygnus Solutions to allow various versions of Microsoft Windows to act similar to a Linux operating system. As AutoDock 3.0.5 is programmed to run on Linux operating system, so for those systems which run on windows, Cygwin is a must. Cygwin consist of two parts: a Dynamic-link library (DLL) as an API compatibility layer providing a substantial part of the POSIX API functionality and an extensive collection of software tools and applications that provide a Unix-like and feel. The completion of autogrid and autodock by the help of Cygwin software is shown in the figure 5.3.

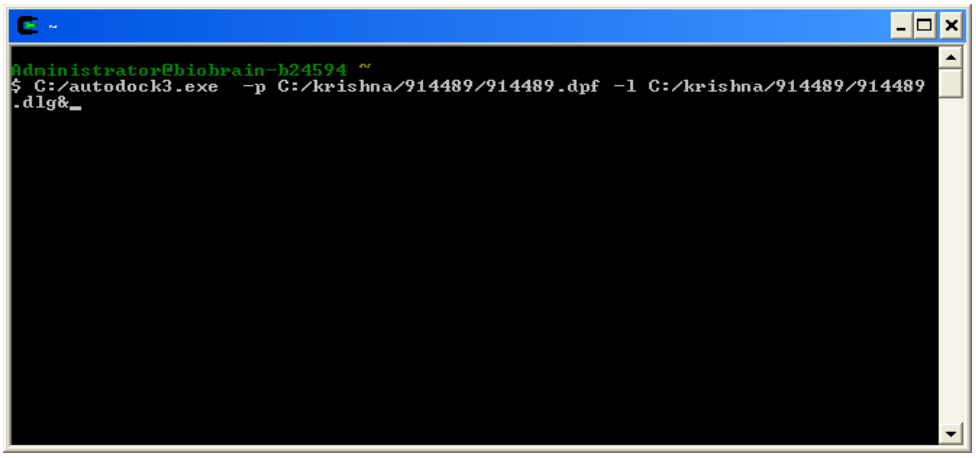

Figure 5.3: Interface of Cygwin

5.1.6 2D QSAR

2D QSAR is basically used to study the biological activities with various properties associated with the structures, which is helpful to explain how structural features in a drug molecule influence the biological activities. The analysis also gathers information that is very much useful for molecular drug design and medicinal chemistry. Therefore correlating the physicochemical properties or structural features of the important compounds with their biological activity is essential. QSAR comprises a numerical set of calculations that help to derive mathematical formulas, which correlate chemical structure and biological activity. QSAR methods numerically represent chemical structures with descriptors and derive the algorithm that can take the mathematical descriptions and formulate some correlation with the increase or decrease of biological performance given to those descriptors. MLR tries to model the relationship between two or more independent descriptors and dependent variable such as IC_{50} by fitting a linear regression equation to the observed data with corresponding parameters (constants) and an error term. Thirty eight known coumarin and alike inhibitors of CK2 (Chilin *et al*., 2008) were used for 2D QSAR studies carried out at the School of Biotechnology, IFTM University, Moradabad, India.

5.1.7 PubChem Compound Database Screening

The PubChem Compound Database (*http://www.ncbi.nlm.nih.gov/pccompound*) contains validated chemical depiction information provided to describe substances in PubChem Substance (Bisen *et al*., 2012**.** Structures stored within PubChem Compounds are pre-clustered and cross-referenced by identity and similarity groups. Snapshot of Pubchem compound database is given below in the Figure 5.4.

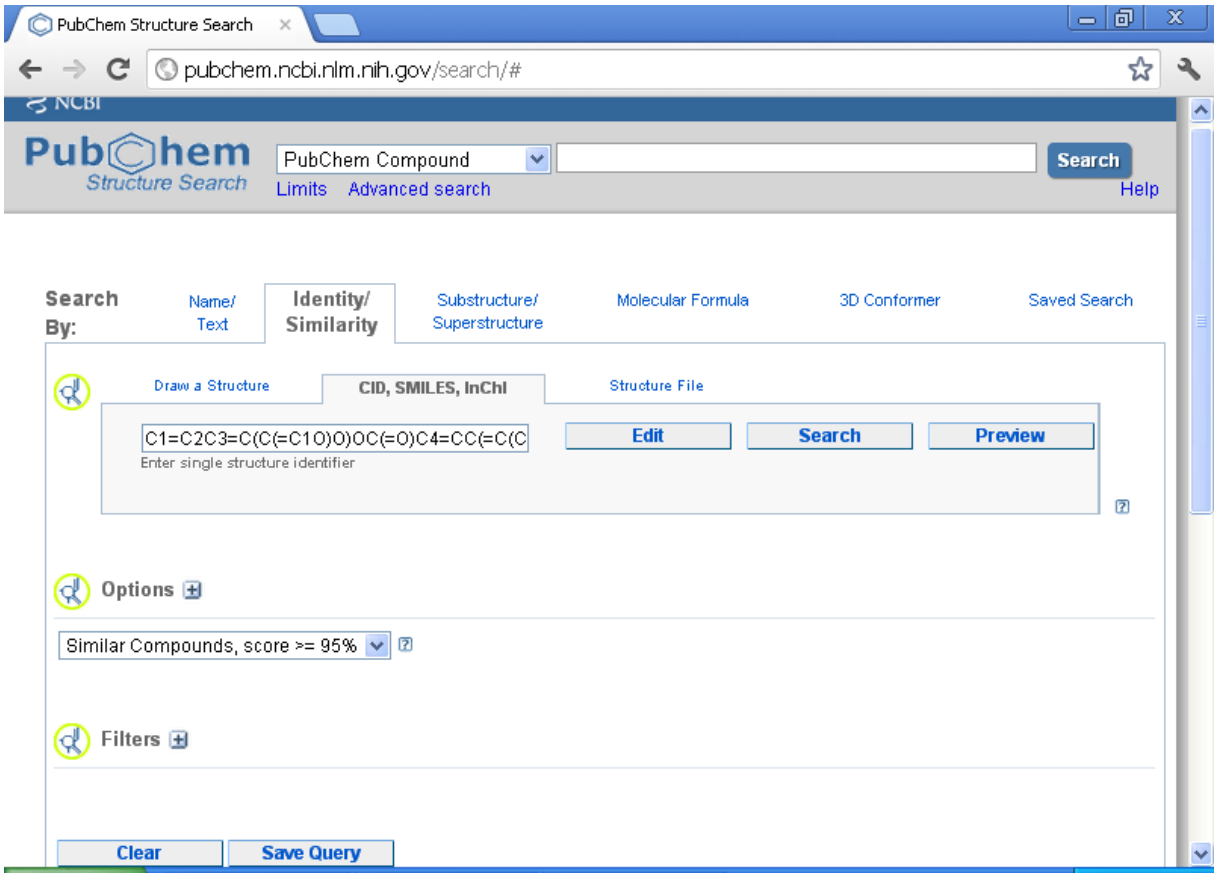

Figure 5.4: Snapshot of Pubchem compound database

A total of 20 analogues of Ellagic acid were screened using the criteria (compounds having similarity value >=95%) for docking studies and docked with CK2.

Table 5.2: Analogues of Ellagic acid.

Sl. N0.	CID No.	Structure	MWT (g/mol)	Molecular formula	X Log P	HBD	HBA
1.	56611575	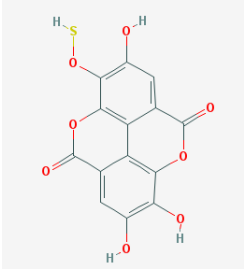	334.25764	$C_{14}H_6O_8S$	1.9	4	9
2	11290032	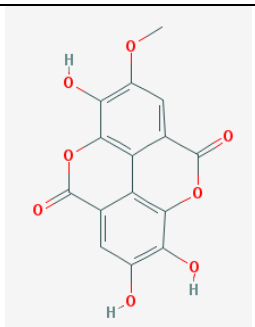	316.21922	$C_{15}H_8O_8$	1.4	3	8
3	15006880	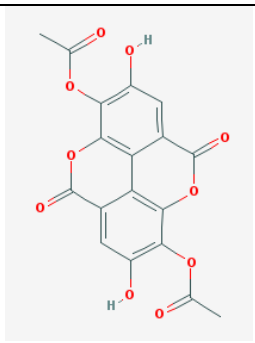	386.266	$C_{18}H_{10}O_{10}$	1.3	2	10
4	53946689	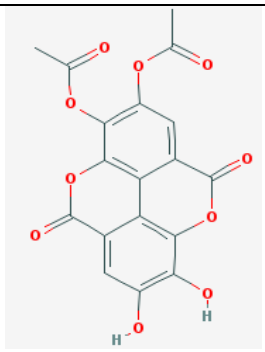	386.266	$C_{18}H_{10}O_{10}$	1.3	2	10

5	5319108	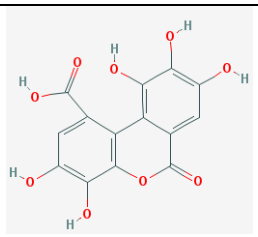	320.20792	$C_{14}H_8O_9$	0.8	6	9
6	5316858	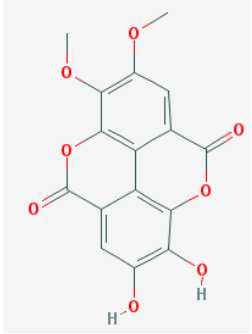	330.2458	$C_{16}H_{10}O_8$	1.8	2	8
7	5491816	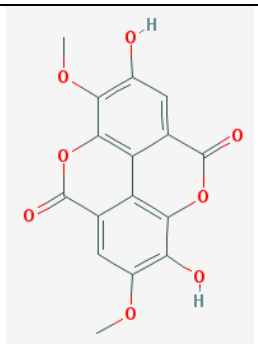	330.2458	$C_{16}H_{10}O_8$	1.8	2	8
8	11580745	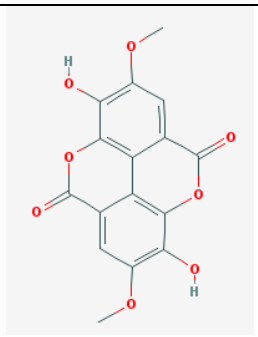	330.2458	$C_{16}H_{10}O_8$	1.8	2	8

9	11674590	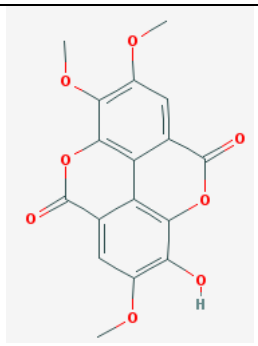	344.27238	$C_{17}H_{12}O_8$	2.1	1	8
10	54122653	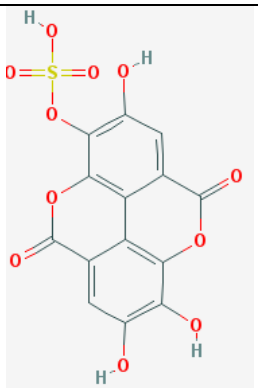	382.25584	$C_{14}H_6O_{11}S$	0.5	4	11
11	46229200	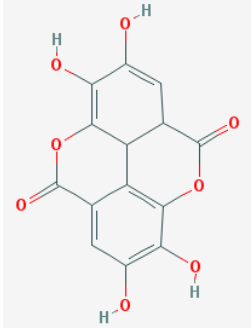	304.20852	$C_{14}H_8O_8$	0	4	8
12	18504424	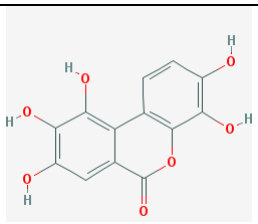	276.19842	$C_{13}H_8O_7$	1.3	5	7

13	10003463	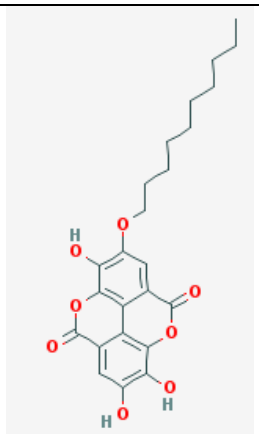	442.45844	$C_{24}H_{26}O_8$	5.9	3	8
14	16049230	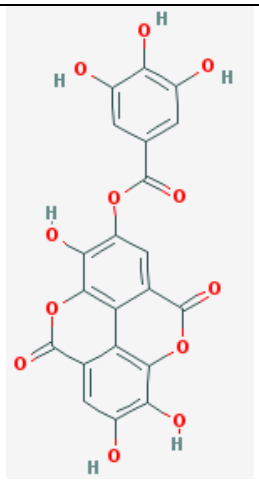	454.2969	$C_{21}H_{10}O_{12}$	1.8	6	12
15	53768212	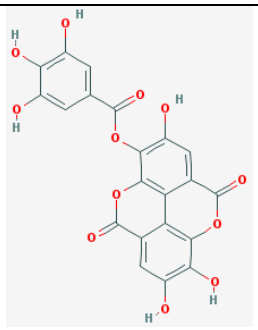	454.2969	$C_{21}H_{10}O_{12}$	1.8	6	12

16	11545697	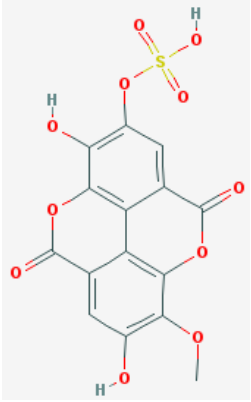	396.28242	$C_{15}H_8O_{11}S$	0.8	3	11
17	14503023	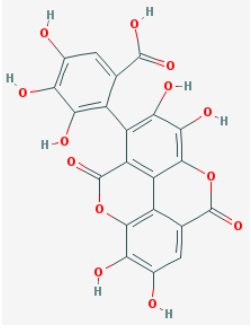	470.2963	$C_{21}H_{10}O_{13}$	1.2	8	13
18	54746813	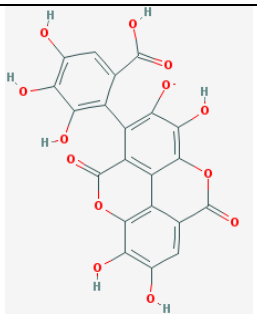	469.28836	$C_{21}H_9O_{13}^-$	1.8	7	13
19	44519391	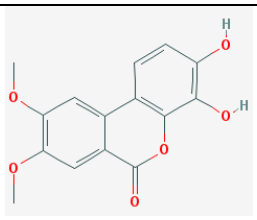	288.25218	$C_{15}H_{12}O_6$	2.3	2	6
20	10400911	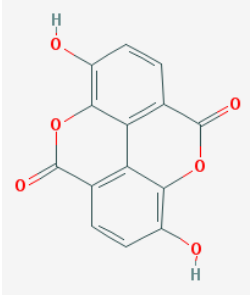	270.19384	$C_{14}H_6O_6$	1.8	2	6

5.1.8 Python Molecular Viewer

Further the best-docked complexes were analyzed through Python Molecular Viewer (PMV) software version 1.5 for their interaction studies. Python Molecular Viewer (Morris *et al*., 1998) is a tool to view the binding of hydrogen bonds in the target molecule. This viewer has most of the features usually expected in a molecule viewer, including a rich set of molecular representations (CPK, sticks, ribbon diagrams, surfaces, etc.), different coloring schemes (by atom, by residue type, by chain, by molecule, by properties, etc.), measuring tools, atom identification by picking, support for multiple molecules, user definable sets of atoms, residues, chains and molecules etc.

5.2 RESULTS AND DISCUSSION

5.2.1 Results of molecular docking

Docking studies predicted the interaction of ligands with protein and residues involved in this complex. For such interaction studies, the most important requirement was the proper orientation and conformation of ligand which fitted to the enzyme binding site appropriately and formed protein-ligand complex. Therefore, optimal interactions and the best autodock score were used as criteria to interpret the best conformation among the 30 conformations, generated by AutoDock 3.0.5 program. The docking results of the known inhibitors with CK2 were shown in Table 5.1 followed by analogues of Ellagic acid as shown in Table 5.2. These data reflect affinity pattern of these potential inhibitors referring to combat against cancer development and proliferation.

5.2.2 2D QSAR

After docking 20 known inhibitors, five types of energy values based descriptors were then used as independent variables for QSAR modeling. Biological activity was expressed in terms of pIC50 (Fig. 5.5 and Table 5.3), the logarithm of measured IC_{50} (μM) against CK2 enzyme. Using linear regression analysis, a QSAR based model was generated using five variables namely Binding Energy (EBind), Intermol Energy (EInterMol), Torsional Energy (ETors), Internal Energy (EEnt) and Docking Energy (DE), which accomplished correlation coefficient r^2 value 0.6617 (Table 5.3). The equation was obtained for the inhibitory activities represented as pIC_{50} values, using the EBind, EInterMol, ETors, EEnt and DE as the variable descriptors. A model with the correlation coefficient (r^2) of 0.3645 was obtained for 38 compounds using the Equation 1.

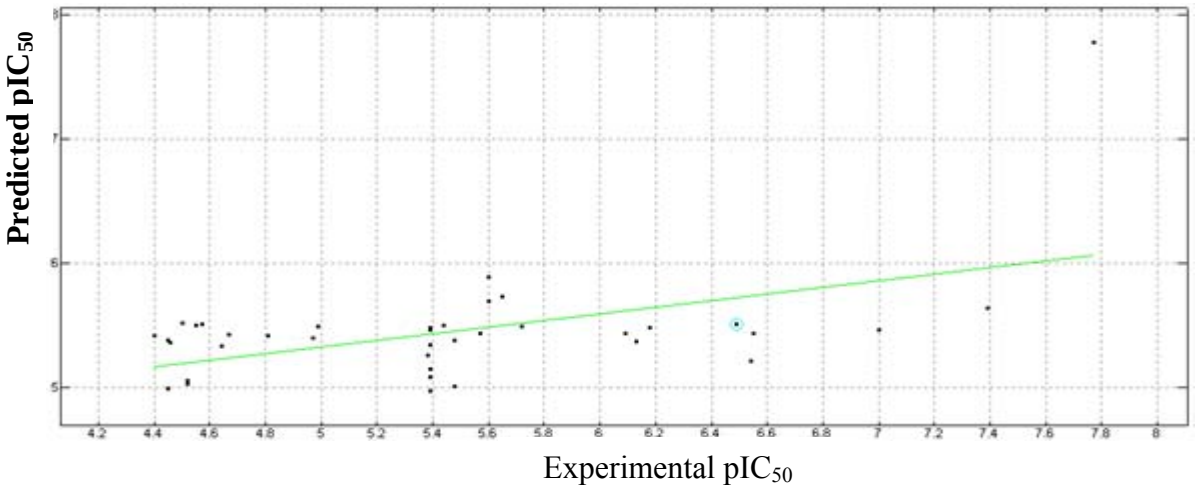

Figure 5.5. Depiction of the experimental and predicted pIC_{50} value in X and Y direction respectively with r^2 value 0.3645 using LINEAR MODEL.

Predicted pIC_{50} = 4.68369 - 0.36245 (DE) -0.07374 (EBind) + 0.32636 (EInterMol) - 0.06069 (ETors) + 1.19649 (EEnt)……(1)

Table 5.3: The experimental and predicted pIC50 values for the training and test set molecules docked with CK2.

Sl. N0.	CID No.	Exp. pIC50	Predicted pIC50	Binding energy (Kcal/mol)	Docking energy (Kcal/mol)	Intermol energy (Kcal/mol)	Torsional energy (Kcal/mol)	Internal energy (Kcal/mol)
1.	54732502	4.40	5.42	-6.48	-60.44	-6.48	0.0	0.03
2	54682226	4.55	5.50	-7.02	-6.97	-7.02	0.0	0.05
3	44456889	6.52	5.20	-2.73	-2.76	-3.05	0.31	0.28
4	44456746	5.44	5.50	-7.41	-7.41	-7.41	0.0	0.0
5	44456745	5.48	5.00	-1.68	-1.83	-2.0	0.31	0.17
6	44456744	5.57	5.43	-7.24	-7.28	-7.24	0.0	-0.05
7	44456718	5.39	5.46	-1.82	-2.11	-2.13	0.31	0.17
8	44456717	5.38	5.25	-6.29	-6.75	-6.6	0.31	0.03
9	44456698	4.97	5.40	-6.16	-6.13	-6.16	0.31	-0.14
10	44456697	4.99	5.48	-7.37	-7.38	-7.37	0.0	-0.01
11	44456695	4.67	5.42	-6.89	-6.91	-6.89	0.0	-0.01
12	44456694	4.69	778	-7.3	-7.77	-7.61	0.31	-0.16
13	44456692	4.64	5.33	-7.5	-8.32	-8.13	0.62	-0.19
14	44456668	4.57	5.50	-6.72	-6.92	-7.04	0.31	0.11
15	44456667	4.50	5.51	-7.25	-7.21	-7.25	0.0	0.04
16	24799273	5.39	5.07	-1.57	-1.57	-1.85	-0.31	0.28
17	24799272	5.48	5.37	-6.93	-7.33	-7.25	0.31	-0.08
18	24799271	5.60	5.88	-6.35	-6.36	-6.98	0.62	0.62
19	24799269	5.39	5.47	-6.9	-6.86	-6.9	0.0	0.04
20	24799087	6.49	5.50	-6.87	-6.9	-6.87	0.0	-0.03
21	24799086	6.55	5.43	-6.78	-6.77	-6.78	0.0	0.01
22	24799081	4.81	5.42	-6.46	-6.43	-6.46	0.0	0.03
23	24799080	5.39	4.97	-1.54	-1.7	-1.85	0.31	0.15
24	24799079	5.60	5.69	-7.21	-7.67	-7.52	0.31	-0.14
25	20144512	5.65	5.73	-6.13	-6.13	-6.13	0.0	0.0
26	15686455	6.13	5.36	-6.2	-6.2	-6.2	0.0	0.0
27	15445625	6.18	5.48	-7.45	-7.48	-7.45	0.0	-0.03
28	13881279	5.72	5.49	-7.11	-7.08	-7.11	0.0	0.03
29	11087876	4.45	4.99	-1.22	-1.32	-1.53	0.31	-0.05

30	5795340	7.00	5.46	-6.86	-6.83	-6.86	0.0	0.03
31	5417177	5.39	5.34	-6.44	-6.8	-6.75	0.31	-0.05
32	5415301	6.09	5.42	-6.64	-6.62	-6.64	0.0	0.02
33	5385113	4.52	5.02	-1.27	-1.46	-1.58	0.31	0.12
34	5376327	5.39	5.14	-1.32	-1.5	-1.63	0.13	0.13
35	5354284	4.45	5.37	-6.06	-6.03	-6.06	0.0	0.03
36	5324654	4.46	5.36	-5.85	-5.81	-5.85	0.0	0.04
37	5291935	4.52	5.06	-1.4	-1.44	-1.71	0.31	0.27
38	5281855	7.39	5.63	-8.72	-8.73	-8.72	0.0	-0.01

5.2.3 Evaluation of QSAR models

To assess the predictive performance of QSAR models, different cross-validation procedures were adopted. First, in leave-one-out strategy (LOOCV), one molecule was removed from the dataset as a test compound and the remaining 37 molecules were used to build the model. This process was repeated 38 times with each inhibitor as a test molecule. Once a regression model was constructed, goodness about the fit and statistical significance was assessed using the statistical parameters. The outcome of results is well described in Table 5.4, which was extracted from the source data as shown in Figure 5.6.

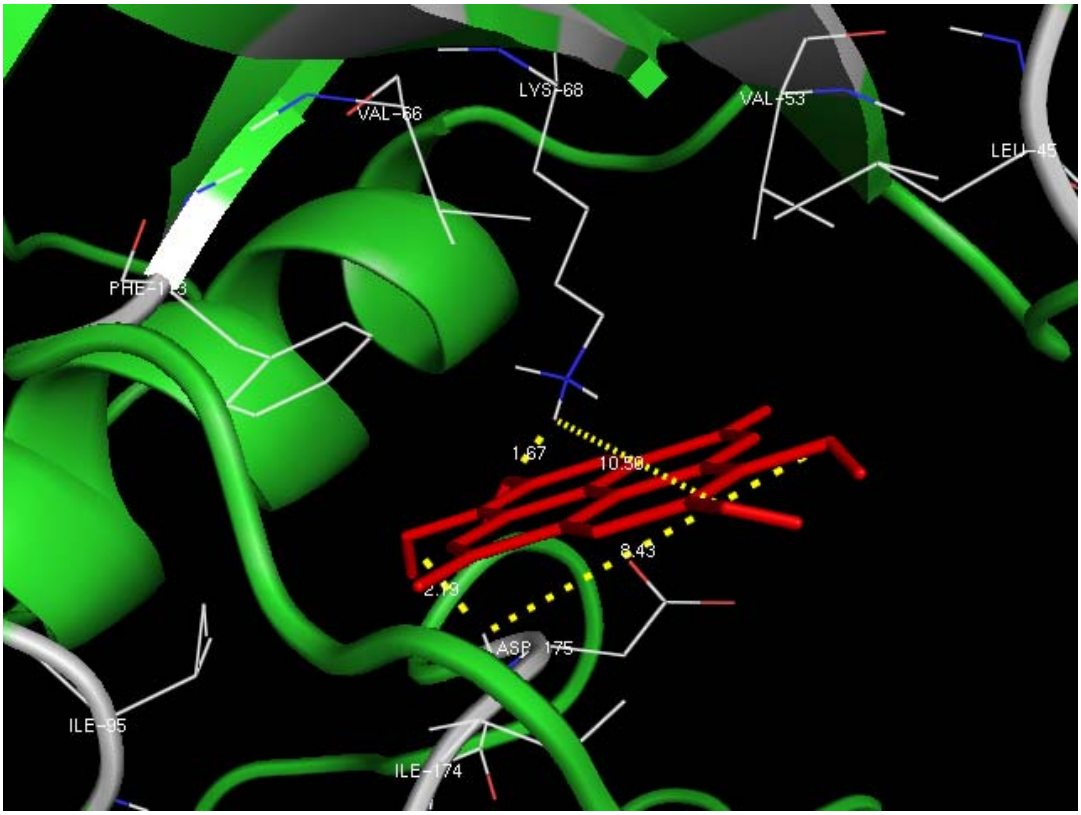

Figure 5.6: Two H-bonds are formed between amino acid LYS68 (HZ3) and ASP175 (HN) with Ellagic acid (O), respectively.

Table 5.4: Activity of newly designed analogues of Ellagic acid based on QSAR model.

l. N0.	CID No.	Predicted pIC50	Binding energy (Kcal/mol)	Docking energy (Kcal/mol)	Intermol energy (Kcal/mol)	Torsional energy (Kcal/mol)	Internal energy (Kcal/mol)
1.	56611575	5.54	-8.52	-8.92	-8.83	0.31	-0.09
2	11290032	5.69	-7.72	-7.83	-8.03	0.31	0.2
3	15006880	5.56	-7.44	-7.66	-8.69	1.25	1.03
4	53946689	6.12	-7.58	-8.07	-8.83	1.25	0.76
5	5319108	4.90	-3.02	-3.45	-3.34	0.31	-0.12
6	5316858	5.76	-7.89	-8.23	-8.51	0.62	0.28
7	5491816	5.82	-7.49	-7.73	-8.11	0.62	0.39
8	11580745	5.71	-6.84	-7.12	-7.46	0.62	0.34

9	1167459	5.26	-6.68	-7.02	-7.62	0.93	0.6
10	54122653	4.68	-3.12	-3.74	-3.74	0.62	0.0
11	46229200	5.74	-9.72	-9.73	-9.72	0.0	-0.02
12	18504424	5.53	-8.14	-8.19	-8.14	0.0	-6.05
13	10003463	5.39	-6.9	-9.97	-10.01	3.11	0.04
14	16049230	5.17	-4.5	-5.43	-5.43	0.93	0.01
15	53768212	5.13	-4.44	-5.39	-5.37	0.93	-0.02
16	11545697	5.05	-1.85	-2.56	-2.79	0.93	0.23
17	14503023	3.88	7.43	6.75	6.81	0.64	-0.05
18	54746813	4.74	-1.56	-2.32	-2.18	0.62	-0.13
19	44519391	5.80	-7.34	-7.57	-7.96	0.62	0.39
20	10400911	5.51	-7.69	-7.72	-7.69	0.0	-0.03

5.2.4 Results of Python Molecular Viewer

A close view of the binding interactions of CK2 with the CID 56611575, CID 46229200 and CID 10003463 were analyzed through Python Molecular viewer and shown below in Figure 5.7, 5.8 and 5.9 respectively. Ligand is highlighted in orange (in stick drawing) and amino acids involved in hydrogen bonds color by atom type.

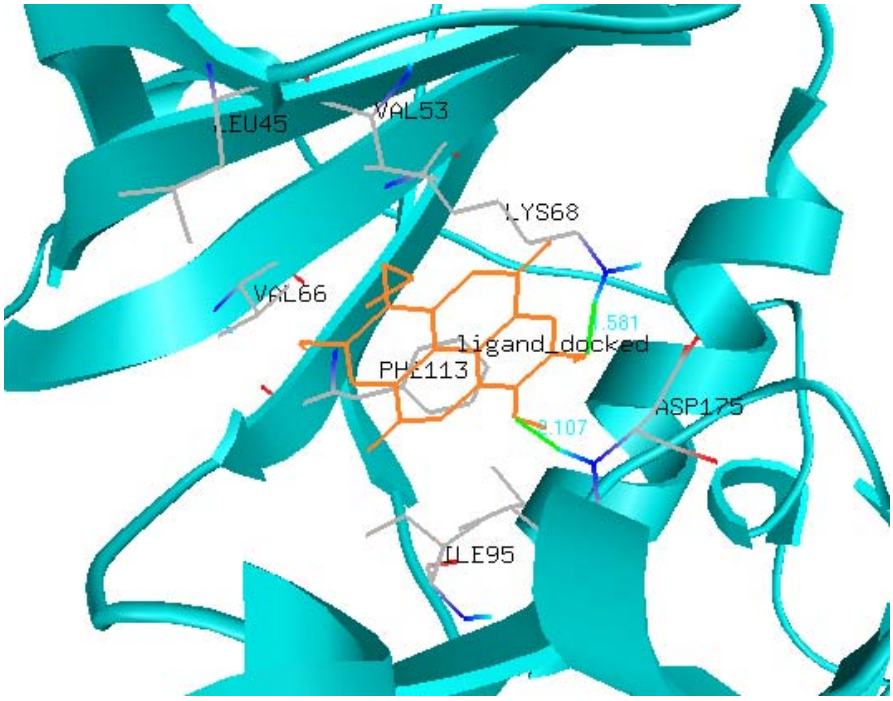

Figure 5.7: Two H-bonds are formed between amino acid LYS68 (HZ3) and ASP175(HN) with compound CID 56611575(O), respectively.

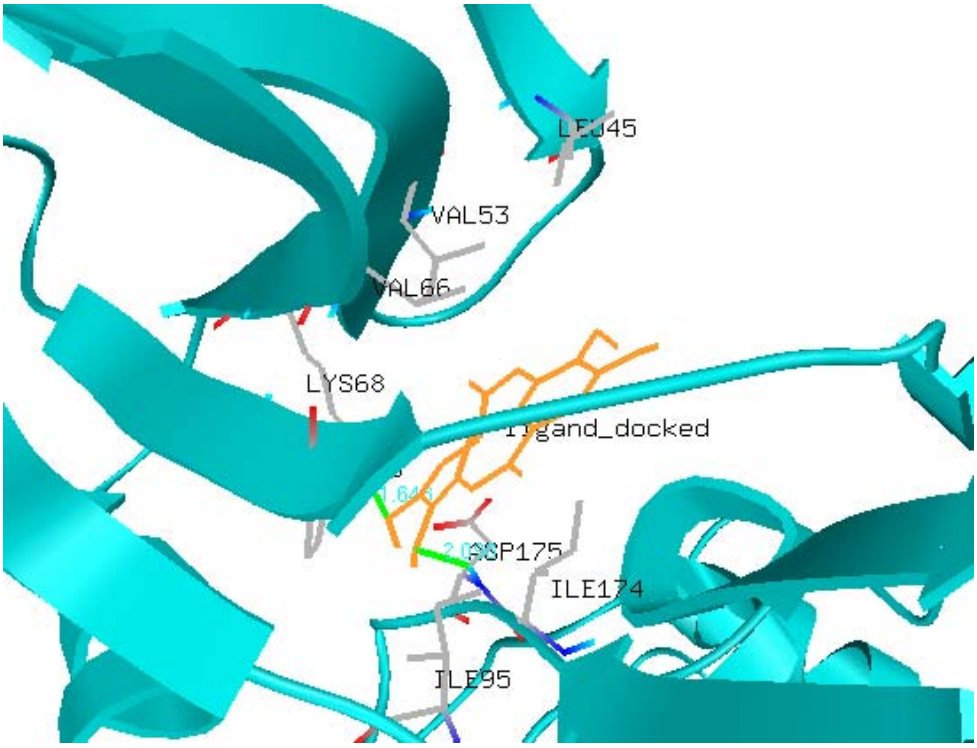

Figure 5.8: Two H-bonds are formed between amino acid LYS68 (HZ3) and ASP175(HN) with compound CID 46229200(O), respectively.

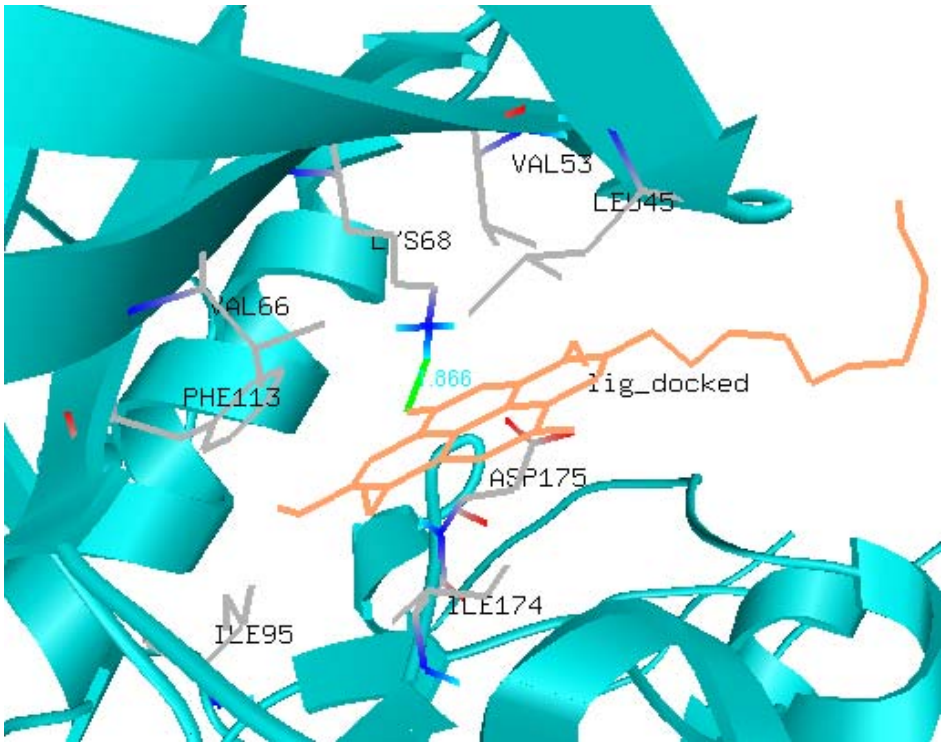

Figure 5.9: One H-bond is formed between amino acid LYS68 (HZ3) with compound CID 10003463(O).

5.3 CONCLUSION

The human casein kinase II (CK2) is a drug targeting protein for the drug discovery fighting with the Oral cancer. Flexible docking of ligand from chemical database to receptor is an emerging approach and is widely used in drug discovery to reduce the cost and time. 38 known coumarin inhibitor of CK2 were used for 2D QSAR study. Using linear regression analysis, a QSAR based model was generated using five variables (descriptors), namely, Binding Energy (EBind), Intermol Energy (EInterMol), Torsional Energy (ETors), Internal Energy (EEnt) and Docking Energy (DE), which accomplished correlation coefficient r2 value 0.3645. After that twenty analogues of ellagic acid were screened from Pub-Chem

compound database and docked with CK2. After docking, three compounds CID 56611575 (--8.92 kcal/mol), CID 46229200 (-9.73 kcal/mol) and CID 10003463 (-9.97 Kcal/mol) had lower docking energy even lower than the standard control Ellagic acid (-8.73 kcal/mol) with CK2. Whether the various pharmacological properties attributed to ellagic acid are due to ellagic acid alone, its metabolites, or the combination of both, is still not precisely known. The anti-proliferative properties of ellagic acid are due to its ability to directly inhibit the DNA binding of certain carcinogens, including polycyclic aromatic hydrocarbons (Teel *et al.*., 1986) and nitrosamines (Mandal *et al.*, 1988; Mandal and Stoner, 1990; Siglin *et al.*, 1995). Ellagic acid down-regulates insulin-like growth factor (IGF-II) (Narayanan and Re, 2001) and activates expression of tumor suppressor genes p53/p21, leading to cell cycle arrest at the G1/S phase and apoptosis (Narayanan *et al.*, 1999). Ellagic acid prevents carcinogen induced tumorigenesis by activating detoxifying enzymes (Barch and Rundhaugen, 1994) and inhibiting certain cytochrome P450 enzymes involved in the generation of mutagens (Zhang *et al*., 1993, Barch *et al.*, 1994). Anticarcinogenic effects of ellagic acid have been reported in prostate (Narayanan *et al.*, 2002), liver (Tanaka *et al.*, 1988), colorectal (Narayanan and Re, 2001), esophageal (Stoner *et al.*, 1999), bladder (Li *et al.*, 2005) and leukemia (Mertens-Talcott and Percival 2005, Hagiwara *et al.*, 2010) cancer cell lines. Ellagic acid was reported to reduce chemotherapy induced toxicity in hormone refractory prostate cancer (HRPC) (Falsaperla *et al*., 2005). Ellagic acid was reported to inhibit 4-nitroquinoline-1-oxide (4-NQO)-induced tongue carcinogenesis in rat (Tanaka *et al.*, 1993) and it also inhibited the growth of premalignant and malignant oral human cell-line (Han *et al.*, 2005).

These three compounds were thus selected as potent candidates leading against cancer. Hydrogen bonding is known to play an important role for the structure and function of biological molecules, especially for inhibition in a complex. These compounds form hydrogen bond with active site residues of CK2. The biological activity of two compounds in terms of IC_{50} were calculated, which could be used as a guideline or reference for anti-cancerous activity of compounds before their synthesis.